Statistics based localized damage detection using vibration response

Siavash Dorvash[*], Shamim N. Pakzad and Elizabeth L. LaCrosse

Civil and Environmental Engineering, Lehigh University, Bethlehem, PA, USA

Abstract. Damage detection is a challenging, complex, and at the same time very important research topic in civil engineering. Identifying the location and severity of damage in a structure, as well as the global effects of local damage on the performance of the structure are fundamental elements of damage detection algorithms. Local damage detection is essential for structural health monitoring since local damages can propagate and become detrimental to the functionality of the entire structure. Existing studies present several methods which utilize sensor data, and track global changes in the structure. The challenging issue for these methods is to be sensitive enough in identifying local damage. Autoregressive models with exogenous terms (ARX) are a popular class of modeling approaches which are the basis for a large group of local damage detection algorithms. This study presents an algorithm, called Influence-based Damage Detection Algorithm (IDDA), which is developed for identification of local damage based on regression of the vibration responses. The formulation of the algorithm and the post-processing statistical framework is presented and its performance is validated through implementation on an experimental beam-column connection which is instrumented by dense-clustered wired and wireless sensor networks. While implementing the algorithm, two different sensor networks with different sensing qualities are utilized and the results are compared. Based on the comparison of the results, the effect of sensor noise on the performance of the proposed algorithm is observed and discussed in this paper.

Keywords: structural health monitoring; localized damage detection; influence-based damage detection

1. Introduction

Structural health monitoring (SHM) plays an integral role in maintaining the integrity of important civil, mechanical, and aerospace structural systems. Structures experience a number of loading scenarios on a daily basis ranging from typical ambient excitations to more extreme wind and earthquake loads. All these loading scenarios may have damaging effects on the structures and, whether the resulting damages are visible immediately or appear more gradually in time, it is important to be able to detect them before they propagate and become detrimental to the functionality of the entire structure and its surroundings. With renewed interest in the deteriorating state of the nation's infrastructure, the need for effective, efficient, and affordable structural health monitoring approaches and maintenance management systems is becoming more and more apparent. A promising approach for monitoring and maintenance management is local damage

---

*Corresponding author, Ph. D., E-mail: sidorvash@gmail.com

detection. Applying this approach helps reduce the cost of repairs by identifying the exact parts of structures that need to be repaired, instead of conservatively retrofitting the entire structure. Additionally, continuous or semi-continuous monitoring of these structures over time will help ensure that they do not fall to serious states of disrepair in the future, which will save on the cost of maintenance in the long term.

Some of the traditional non-destructive evaluation (NDE) techniques, listed in ASM Handbook (Anon. 1992) include but are not limited to visual inspection, liquid penetrant (Deutsch 1979), eddy currents (Banks *et al.* 2002, Ziberstein *et al.* 2003), ultrasonic waves (Mallet *et al.* 2004), acoustic emission, and infrared thermography (Trimm 2003, Ball and Almond 1998). While these methods can be useful in certain circumstances, their success is dependent on a prior knowledge of potential damage location (Doebling *et al.* 1998). Also, for application of these methods, it is necessary to have direct access to the location of damage, which may be a difficult task, especially after an event such as an earthquake. Furthermore, NDE techniques are costly and labor-intensive.

Advancements in sensing technology have allowed for the development of new SHM methods that can be applied on a temporary or semi-permanent basis for continual monitoring of structures (Lynch and Loh 2006, Farrar *et al.* 2005). One example of improvements in sensing technology is application of wireless sensor networks which have made instrumentation of sensing techniques more affordable and with minimal labor demand (Lynch *et al.* 2004, Pakzad *et al.* 2008, Jang *et al.* 2010, Gangone *et al.* 2011, Dorvash *et al.* 2012). An application which benefits from advancements of sensing and instrumentation technologies is vibration-based SHM which is commonly used to extract the dynamic characteristics of the structure from its response (Whelan and Janoyan 2009, Cho *et al.* 2010, Kim *et al.* 2010, Yu *et al.* 2010, Jang *et al.* 2010). Literature presents numerous damage detection methods which rely on changes in identified dynamic characteristics (e.g., natural frequencies, mode shapes, and modal damping) to reveal changes in the physical properties of the structure (e.g., mass and stiffness), i.e., structural damage (Doebling *et al.* 1998, Alvandi and Cremona 2006). While the concept may be intuitive, application of methods which rely on dynamic characteristics of the structure are not without obstacles. Modal properties are indicators of the global state of the structure and are not sensitive enough to local damages (Farrar *et al.* 1994, Chang *et al.* 2003). Therefore, these methods are mostly referred to as global-based damage detections. Also, some SHM practices involving global-based damage detection require knowledge of specific structural properties, including mass, stiffness, or damping ratio, for which it is often difficult to determine very accurate estimates (Koh *et al.* 1995, Morassi and Rovere 1997, Sohn and Law 1997, Ratcliffe 1997). On the other hand, local damage detection is desired for structural health monitoring since local damages happen first and can propagate to the entire structure.

Literature also presents some effective local damage detection methods, such as damage locating vector (DLV) method (Bernal 2002, Sim *et al.* 2008, Sim *et al.* 2011) and two-dimensional gapped smoothing method (Yoon *et al.* 2005). While effective, these methods have some requirements. For example DLV method requires the knowledge of structural properties, or requires homogeneity of the structural properties as in the two-dimensional gapped smoothing method. In addition, considering the current state of damage detection techniques in practice, more research is still needed to improve existing algorithms, develop more effective techniques, and make damage detection more practical and applicable in real-life monitoring scenarios. In this regard, this paper presents an effective damage detection method, called Influence-based Damage Detection Algorithm (IDDA) that uses vibration responses to achieve localized damage detection without the need for exact knowledge of structural properties. The method is based on regression

of the vibration response and estimation of influence coefficients as damage indicators. (Dorvash *et al.* 2014, Shahidi *et al.* 2014, Yao and Pakzad 2014). While the algorithm is effective, it is also very practical as it converts the shear amount of time-history data into condensed information which enables detection of structural changes in the system.

In IDDA, *influence coefficients*, as defined in section 2, obtained from linear regression between every two node responses, are used as the index for determining and detecting the occurrence of changes in the structural properties. The change point of time-variant influence coefficients is also determined using a Bayesian statistical framework (Pakzad 2008). The effectiveness of the proposed local damage detection method is demonstrated and verified through simulated and experimental results. For the experimental implementation of the algorithm two different networks of wired and wireless sensors are utilized and the results of the two sensor networks with different noise characteristics are evaluated and compared to observe the effect of sensor noise on the effectiveness of the algorithm.

2. Localized damage detection method

This algorithm bases its damage detecting capabilities on the premise that a structure's response changes when physical properties change, i.e., due to damage. The response of the structure is monitored at various locations via a spatially dense sensor network, and linear regression influence coefficients are extracted. When damage occurs, this linear relationship changes, which is reflected in the influence coefficients indicating the existence of damage. In addition to identifying that damage has occurred, considering the locations of sensors associated with changing coefficients allows for localization of the damage as well. Furthermore, a statistical framework that utilizes hypothesis testing can be implemented to determine whether damage exists at a significant confidence level.

2.1 Structural model

Damage detection methods can be classified in a number of ways. One common classification is as identification of linear or nonlinear damage. The definition of linear damage is "the case when the initially linear-elastic structure remains linear-elastic after damage" (Doebling *et al.* 1998). One advantage of studying a linear damage state is that the linear equations of motion still apply after damage. The method proposed in this work relies on this assumption of linearity before and after damage.

In order to demonstrate the linear-elastic assumptions of this method, a rigid beam-column joint is considered, as shown in Fig. 1. The general free body diagram has 9 unknowns (x_i, y_i, r_i, x_j, y_j, r_j, x_k, y_k, and r_k) assuming the joint to be restrained out-of-plane. The displacement at any point along the structure, u_n, can then be defined as a function of each of these unknowns as follows

$$u_n = f(x_i, y_i, r_i, x_j, y_j, r_j, x_k, y_k, r_k) \tag{1}$$

Because the joint represents a small portion of the structure, the member lengths create small angles. Small angles correspond to negligible rotations reducing the number of degrees of freedom (DOFs) to 6 independent translational DOFs (x_i, y_i, x_j, y_j, x_k, and y_k). This number of DOFs can be further reduced with the practical assumptions of inextensibility of the column and beam members.

A structure that is being monitored will experience excitations of the ambient type for a majority of its useful life. Other more extreme excitations should be considered as occurring during the damaging event, in which case the linearity assumption does not hold true. Because this method involves the comparison of the structural state pre- and post-event, as opposed to during the nonlinear damaging event, it is reasonable to consider the structure within a linear-elastic range. Thus it is valid to consider Eq. (1) as a linear function.

Another important assumption for the application of this method is that the contributing mass at the considered portion of the structure is negligible. This assumption allows local dynamic effects to be neglected such that the structure can be considered in its linear static state (Pakzad 2008 and Chang and Pakzad 2014, Dorvash et al. 2014). Both found that because the stiffness of elements forming the connection is much larger in comparison to their contributory mass when considering a local portion of the structure, the effect of the mass term becomes negligible and the dynamic equation of motion can be reduced to a static relationship. However, it is important to note that this assumption only applies to a local joint. Therefore, the linear relationship between nodes that are within the same local joint and share a relatively stiff portion of the structure should be assessed for this algorithm. This may translate to small clusters of dense sensor networks within a larger-scale instrumentation network.

Considering this small portion of the structure (the beam-column connection) as a linear static system, any displacement response along the connection is a linear function of the response at other locations and the relationship between the responses at any two locations, nodes i and j, can be defined as

$$u_j(n) = \beta_{ij} + \alpha_{ij}.u_i(n) + \varepsilon_{ij}(n) \tag{2}$$

where, $u_i(n)$ and $u_j(n)$ are structure's response at nodes i and j, respectively, and at time n, β_{ij} is intercept value of regression between nodes i and j, α_{ij} is influence coefficient of regression between nodes i and j, and ε_{ij} is the residual of the regression model.
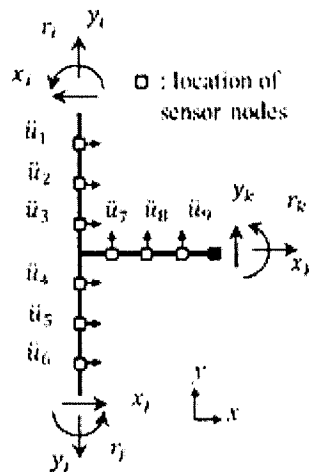

Fig. 1 Free body diagram of a rigid beam-column joint

2.2 Mathematical model

The relationship between responses at different locations of a structure can be established using an Auto Regressive with Exogenousterm (ARX) model as follow

$$\sum_{p=0}^{P} a_p y(n-p) = \sum_{q=1}^{Q} b_q x(n-q) + \varepsilon(n) \tag{3}$$

where y and x are output and input respectively, a_i's and b_i's are ARX coefficients, $\varepsilon(n)$ represents the residuals, n is the time index, and P and Q are orders of the autoregressive and exogenous parts of the ARX model, respectively. Based on this mathematical representation, the response at any time step can be estimated having the past inputs and outputs and the current input.

In a linear structural system, each output is a linear function of input excitations and therefore, the linear relationship holds between different outputs and the ARX model can be written to correlate outputs as follow

$$\sum_{p=0}^{P} a_{jp} y_j(n-p) = \sum_{i=1}^{k} \sum_{q=0}^{Q} b_{iq} y_i(n-q) + \varepsilon(n) \tag{4}$$

where output at node j is related to current and previous outputs at nodes $i = 1$ *to* k. This equation establishes a relationship between one output and other outputs of the system. The accuracy of this model depends on the selected model orders. While higher model orders, in general, deliver more details of the system and reduce the estimation bias, it is always desired to keep the order at the minimum level to avoid over-parameterization. Considering the special case of the linear system with negligible mass (absence of inertia force),described in the previous section, the corresponding ARX model can be developed by assuming P and Q equal to zero

$$y_j(n) = \sum_{i=1}^{k} \frac{b_i}{a_j} y_i(n) + \beta_{ij} + \varepsilon(n) \tag{5}$$

which correlates the response at node j to current responses at nodes$i$ $(= 1$ *to* $k)$. Addition of intercept (β) into Eq. (5) is in order to account for the initial condition, since the effects of previous time steps are removed from the equation. Note that Eq. (5) represents a multi-variable version of Eq. (2) (i.e., considering $k = 1$ and $b_i/a_j = \alpha_{ij}$, the same equation will be obtained).

2.3 Influence coefficients as damage indicators

IDDA takes responses of the structure and uses the assumed linear relationship between different nodes, or sensor locations, with one another. By calculating influence coefficients, α_{ij}, between two nodes i and j, based on vibration-induced acceleration response data, the correlation between these responses is determined according to Eq. (2).

The comparison of the resulting influence coefficients from the initial undamaged state with that of the damaged state of the structure serves as a "damage indicator" when it yields a significant change in the value of the coefficients from state to state. More specifically, the influence coefficients exhibit a much more significant change when nodes i and j are located on opposing sides of the damaged segment versus when they are on the same side. From linear regression, this translates to a change in the value of α_{ij} from that of the original undamaged case.

This characteristic allows for the identification of the damage location by inspection of the pattern in which influence coefficients exhibit significant changes.

2.4 Influence coefficient accuracy and estimation error

Once the coefficients are estimated, the accuracy of the data must be assessed and verified before damage detection can be performed. This is done through consideration of both the accuracy of the pair-wise coefficients and the estimation error. The product of influence coefficients α_{ij} and α_{ji}, yields the evaluation accuracy, EA_{ij}, of these coefficients, indicating which node responses are linearly related to one another with the least amount of error, ε_{ij}, and thus are more accurate predictors. An evaluation accuracy of 1.0 signifies a strong accuracy of estimation, while a product of less than 1.0 corresponds to progressively higher values of noise and nonlinear behavior of the physical structure.

The second parameter that is used for data verification is normalized estimation error, which is calculated by

$$\gamma_{ij} = \frac{\sigma_{\alpha ij}}{\alpha_{ij}} \tag{6}$$

where α_{ij} is influence coefficient between nodes i and j and $\sigma_{\alpha ij}$ is standard error of the influence coefficient estimates α_{ij} and can be estimated by the following equation

$$\sigma_{\alpha ij} = \frac{\sigma_{\alpha ij}}{(\sum y_i^2)^{1/2}} \tag{7}$$

In Eq. (7), σ_e is the standard error of the residuals, e (the difference between the estimated and true response).

Normalized estimation error allows for a direct comparison of the amount of error associated with the estimation of each influence coefficient as a damage indicator. A low estimation error, resulting from a low standard error of the estimated influence coefficient, will correspond to a more accurate predictor. Once the accuracy and error have been assessed for each coefficient, post-processing of the best influence coefficients can be performed for damage identification and localization.

When the influence coefficients have been assessed for accuracy and error, the most reliable of these are chosen for use in damage detection. As was previously discussed, changes in the physical properties of the structure, such as loss of material stiffness or change in boundary conditions due to damage, are reflected in changes in the behavior of the structure which can also be seen directly in the influence coefficients; the linear relationship between certain locations of the structure will change to differing degrees depending on the location of the damage. The degree to which certain coefficients change can indicate the location of the damage.

2.5 Statistical framework

In order to determine what defines a "significant change" in the influence coefficients, a statistical framework has been developed and applied. This framework is useful for processing large volume of data as a structure is monitored over time. A *Bayesian Statistic* is used to

determine the change point, the point at which the data indicates damage, at a 95% confidence level (Chen and Gupta 2000). This statistical inference method tests the hypothesis that the mean of the influence coefficients for each successive test is equal to the mean of the influence coefficients from the initial undamaged state.

$$H_0 : \alpha_1 = \alpha_2 = \cdots = \alpha_N = \overline{\alpha} \tag{8}$$

Eq. (8) defines null hypothesis, H_0, which assumes that the mean of the influence coefficients is unchanged. This is tested against the one-sided alternative hypothesis, H_A, where assumes that the values of the influence coefficients beyond the change point, denoted as r, are greater (or smaller) than that of those prior to this point by a significant amount

$$H_A : \alpha = \alpha_1 = \cdots = \alpha_r < \alpha_{r+1} = \cdots = \alpha_N \tag{9}$$

where N represents the number of tests. The change point r, mean μ, and standard error σ of the influence coefficient are all unknown. The statistic that is developed to test the aforementioned hypothesis is a Bayesian statistic as follow

$$S_N = \sum_{i=r}^{N-1} i \cdot (\alpha_{i+1} - \overline{\alpha}) \tag{10}$$

where r, the change point, can be any point from 1 to $N - 1$. This Bayesian statistic, in fact, assigns a weight (i) to changes that happen successively. In other words, as the offset in the mean value of the influence coefficients persists, the difference between the mean and the baseline will be accumulated by increasing factors. To test the significance of change and conclude the alternative hypothesis, H_A, with a certain confidence level, the following normalized t-statistic is utilized

$$t = \frac{S_N}{\sigma \cdot \sqrt{\dfrac{N(N-1)(2N-1)}{6}}} \tag{11}$$

where $\hat{\sigma}$ is the estimated error of the influence coefficient and the denominator of the equation is the deviation of S_N. The test statistic t, has a t-distribution with $N - 2$ degrees of freedom (Sen and Srivastava 1975). In this work, the hypotheses are tested at a 95% confidence level.

The physical significance of this hypothesis testing is such that the alternative hypothesis, H_A, indicates that the structure has incurred damage, while the null hypothesis, H_0, means that there is not adequate evidence to establish that damage exists. These hypotheses are tested for those node pairs that have been identified as significant damage indicators in the assessment and verification stage of the method.

Influence-based damage detection algorithm with its different steps is outlined in Fig. 2. There are three phases in the implementation of this algorithm: (i) data retrieving and parameter extraction, (ii) validation and accuracy assessment, and (iii) post-processing and decision making. The next sections of this paper will present the implementation of the algorithm on different simulated and experimental models.
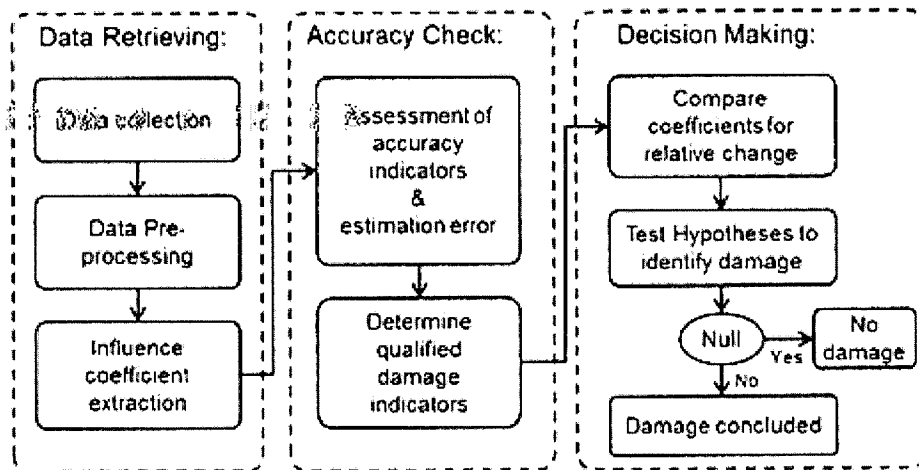
Fig. 2 Methodology for damage detection

3. Simulated beam-column connection

Since IDDA is developed for detection of local damages, the evaluations are presented based on a beam-column connection (which is a local and also a critical structural element) as a testbed structural component. In this section, IDDA is validated using a simulated model of the beam-column connection with 1.8 (m) length for column, 0.9 (m) length for beam, and cross section of 25 (mm) square hollow tube with a wall thickness of 3 (mm) and modulus of inertia equal to 23711 (mm^4). The finite element simulation is created using SAP2000. The beam-column shown in Fig. 1 represents a localized portion of a larger structure, for example a single joint in a larger building frame. A joint is a location in a structure that is prone to damage due to high stress concentrations at the connections. The ability to determine not only the joint, but the location within the joint where damage has occurred can lead to more efficient and cost-effective repair solutions in a structure.

The column portion of the joint is fixed at both ends while the beam cantilevers out from the centerline of the column. Two simulation conditions are performed which include (1) an undamaged baseline condition and (2) a damaged condition, characterized by a reduction in the beam stiffness (15% reduction in stiffness). For each of these models, acceleration response is simulated at each of the 9 nodes for a white noise excitation applied at the free end of the beam in the y-direction. Measurement noise is accounted for by adding a Gaussian noise with a standard deviation equal to 5% of the root mean square (RMS) of each response signal. Fig. 3 shows the schematic of the simulated beam-column connection and the acceleration response at two nodes before and after the damage is applied.

The influence-based damage detection algorithm is then applied to the simulated data and the parameters are extracted. The relative changes in the influence coefficients between the undamaged and damaged states are shown for each pair-wise node relationship in Table 1. The influence coefficients α_{ij}, $1 \leq i, j \leq 6$ all experience very small (less than 5%) changes

between the undamaged and damaged states. This implies that the physical properties between these nodes have not changed significantly. However, the coefficients of nodes 1 through 6, paired with nodes 7, 8, and 9 show relative changes of between 20-30%. When nodes are on opposite sides of the damage, i.e., nodes 1 through 6 are located on the undamaged column, while nodes 7, 8 and 9 are located on the damaged part of the beam, the physical properties between the paired nodes changes. This physical change is reflected in a more significant relative change in the value of influence coefficients. Furthermore, the influence coefficients α_{ij}, $7 \leq i,j \leq 9$ also experience a noticeable change in coefficients (about 5-10%). This signifies that the physical properties of the structure between the nodes associated with α_{78}, α_{79}, and α_{89} have changed. Therefore, damage is more likely to exist between these nodes. This is consistent with the simulated damage which was applied by stiffness reduction of the beam.
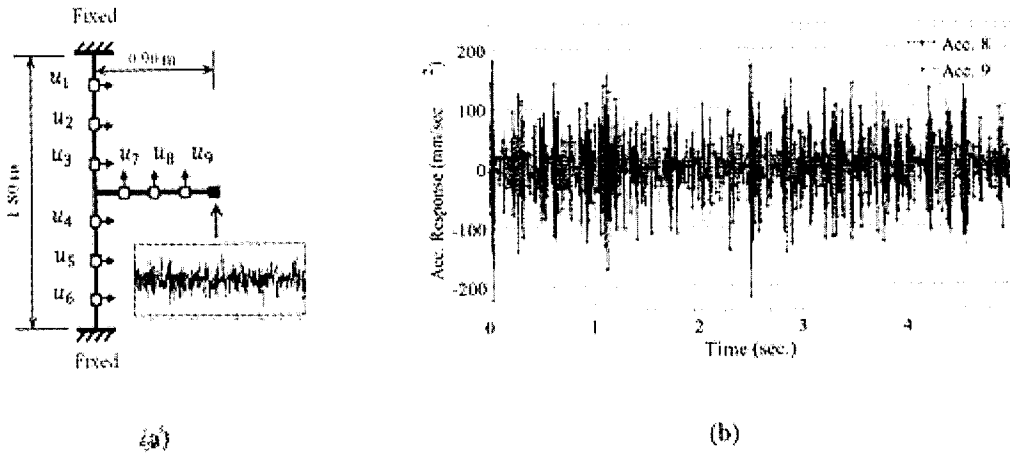

Fig. 3 (a) Simulated model and (b) Acceleration response in undamaged states

Table 1 Relative change in influence coefficients, α_{ij}, from undamaged to damaged states for simulated structure

Node	1	2	3	4	5	6	7	8	9
1		-2.52	-2.98	-5.47	-6.09	-4.36	23.38	26.90	19.65
2	0.03		-0.62	-1.24	-0.99	-0.80	15.20	15.59	45.37
3	0.38	-0.25		-1.16	-0.39	-0.47	30.94	14.91	22.18
4	0.73	0.26	0.18		0.16	0.04	11.57	41.78	27.38
5	0.03	-0.76	-0.94	-1.54		-0.51	12.45	15.50	20.46
6	-2.30	-2.20	-3.99	-6.58	-3.98		26.69	25.47	20.65
7	-12.24	-9.60	-15.14	-13.13	-11.98	-25.28		6.00	12.41
8	-15.90	-15.06	-17.73	-19.65	-19.95	-13.48	-5.82		5.37
9	-33.70	-23.31	-25.59	-13.27	-33.58	-16.35	-8.56	-6.60	

While functionality of the algorithm is showed throughout this example, its performance still needs to be evaluated throughout experimental data. The next section shows the implementation of IDDA, including accuracy assessment, post-processing and decision making steps, on a beam-column connection model constructed in the laboratory.

4. Experimental beam-column connection

IDDA is further verified through implementation on a laboratory beam-column connection model. The prototype represents a portion of the beam and column members as they come to a local joint. The small-scale experimental prototype was constructed with the same dimensions as the simulated model (1.8 [m] length for the column member, 0.9 [m] length for the beam member with 25 [mm] square hollow tube cross section with a wall thickness of 3 [mm]).The specimen is tested for both an undamaged and a damaged state. To simulate damage in the location of the connection joint, the beam member was switched out for a member of lesser wall thickness (corresponding to a 40% stiffness reduction).Note that this just represents a reduction in stiffness near the connection and not the entire beam element.

To generate acceleration responses, the free end of the cantilever is attached to an actuator and excited by harmonic force at 15 Hz frequency with amplitude resulting in 40 mg acceleration at sensor location 9. The wired data is collected at a 250 Hz sampling rate with each test lasting 40 seconds. The wireless data is collected with the same length as wired data. Using both wired and wireless sensors, the data collection is performed simultaneously for direct comparison. The undamaged and damaged structures are each tested 15 times. The collected data samples are then processed through IDDA to detect the occurrence of damage. The results of the implementation of the algorithm using wired sensors are presented in this section and the comparison of sensor network results are discussed in the next section.

The structure is instrumented with two sensor networks with different noise levels of the accelerometers; wired and wireless accelerometers each including 9 sensors, as shown in Fig. 4. The wireless accelerometers used in this implementation consist of Imote2 processing board produced by Intel (2005) combined with SHM-A sensor board, integrating tri-axial LIS3L02AS4 (STMicroelectronics 2005) accelerometer with 50 $\mu g/\sqrt{Hz}$ noise density, developed by Rice and Spencer (2008, 2009). The wired sensors, on the other hand, are capacitive accelerometers (PCB3701, Piezotronics, Inc. 2004) with 3 $\mu g/\sqrt{Hz}$ noise density. Due to lower noise level of wired sensors and the more reliable network, the wired results are used as a direct comparison point for the wireless sensors. Table 2 shows the specifications of the two accelerometers used in the two sensor networks of this study. The reason for having two sensor networks is to assess the effects of sensing network quality on the damage detection process and the level of confidence for decision making.

Table 2 Specifications of the two accelerometers used in the two sensor networks of the experiment

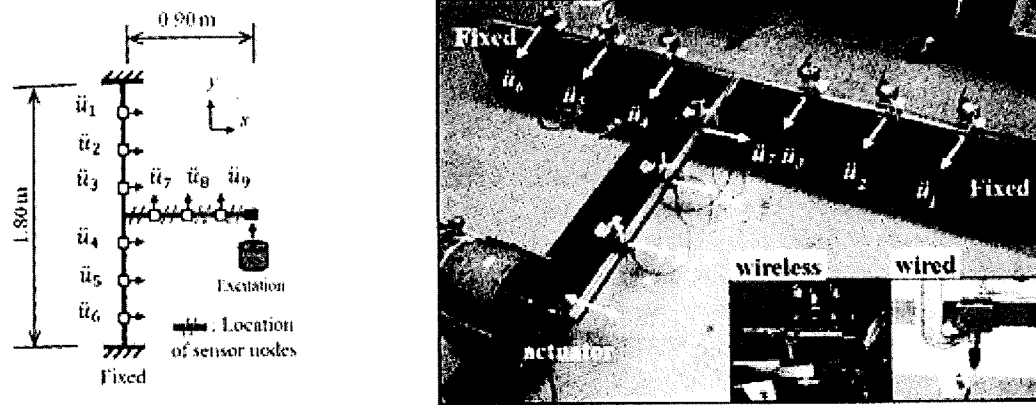| Parameter	LIS3L02AS4	PCB 3701
Acceleration range	±2 g	±3 g
Output noise	50 micro-g/√Hz	3 micro-g/√Hz
Sensitivity	0.66 v/g	1.00 v/g
Temperature Range	-40 to 85°C	-40 to 85°C

Fig. 4 Experimental test bed for beam-column prototype instrumented with wired and wireless accelerometers

4.1 Accuracy assessment and verification of influence coefficients

Having 9 sensors, 72 influence coefficients can be obtained by performing linear regression and presented in Table 3. Once the coefficients have been calculated from the acceleration data, the estimates must be assessed to identify the most significant indicators, which can then be used for damage detection. The evaluation accuracy, EA and estimation error,$\gamma$are integral for this accuracy assessment. By inspection of these parameters, different trends can be identified in the undamaged and damaged parameters, with different estimation errors and evaluation accuracies. The identified trends are associated to the location of node pairs on the structure. Identifying these trends allow classification of nodal pairs and the associated accuracy parameters of their influence coefficients into six different groups based on the values of EA and γ, as presented in Table 4. In this table, the average accuracy of pairs at different regions is rated from high to low and their corresponding locations are presented to describe the reason for different accuracies. Region 1 in the table corresponds to the least estimation error and highest accuracy, and region 6 corresponds to the greatest estimation error and lowest accuracy. Therefore, parameters in region 1, consisting of α_{ij}, $7 \leq i,j \leq 9$, are the most accurate and have the least error. This is a reasonable outcome as the actuator applies force at the end of the beam, closest to nodes 7, 8, and 9. This proximity and boundary condition result in larger amplitude of excitation at these nodes compared with that of the column nodes, thus, corresponding to a higher signal-to-noise ratio (SNR) of the data at these nodes. A higher SNR correlates to better quality data and more accurate results.

On the contrary, region 6, which consists of parameter α_{16}, exhibits the poorest accuracy and the greatest estimation error. This can be accounted for by the fact that each of these nodes is located at either end of the column near the fixed ends. These boundary conditions restrict the column from movement closest to the support, greatly reducing the magnitude of the acceleration signal and thus, the SNR of these nodes. Figs. 5(a)-5(f) show examples of $\alpha$from different regions and their corresponding EA and γ. Fig. 5(a) shows that EA is almost equal to unity and γ is almost equal to 0 for region 1. The EA and γ values for a region 3 pair, shown in Fig. 5(c) also exhibit accurate values, although not quite as accurate as region 1. Fig. 5(f), however, shows a

much lower EA and a noticeably higher γ associated with region 6. Based on similar data for all 6 regions, it can be concluded that regions 1 through 3 contain the most accurate data and thus the most useful damage indicators. On average, these influence coefficients exhibit accuracy greater than 98% and estimation error less than 0.2%.

4.2 Post processing and damage detection

Based on the accuracy assessment, region 1, 2, and 3 coefficients are considered for damage detection. Fig. 6(a) shows the average percent changes of a few pair-wise coefficients in different regions on their corresponding locations. This further supports the theory that nodes on opposite sides of damage show the greatest change, while nodes with no damage between them show a significantly smaller change. Pairs with nodes within the damage location show some change, but not as large as that of nodes on opposite sides. The reason for this is that when both nodes are within the damaged area, both nodes experience similar increases in flexibility, resulting in a less severe differential. Therefore, inspection of the pattern of changes in pair-wise coefficients points to the location of damage within the structure (i.e., damage between nodes 2 and 7, 3 and 8, and so forth).

Table 3 Relative change in influence coefficients, α_{ij}, for experimental structure

Node	1	2	3	4	5	6	7	8	9
1		2.91	5.22	8.57	2.26	1.37	16.65	27.39	31.76
2	2.16		1.21	12.75	6.36	6.40	21.44	32.65	37.22
3	4.15	1.10		13.22	6.96	7.19	22.56	33.91	38.54
4	12.17	15.04	16.64		6.44	6.87	4.63	14.24	18.12
5	5.67	8.62	10.21	6.68		0.22	12.21	22.50	26.65
6	7.09	9.17	10.59	5.51	0.86		11.36	21.55	25.64
7	15.54	18.10	19.24	6.35	11.93	12.03		9.28	13.06
8	22.78	25.11	26.13	14.40	19.51	19.62	8.52		3.49
9	25.44	27.67	28.65	17.37	22.30	22.42	11.63	3.38	

Table 4 Trend regions according to average estimation error (γ) and evaluation accuracy (EA)

| Region	Influence Coefficients	Location of pairs on the beam-column connection model	γ_{ij} Average	EA_{ij} Average
1	α_{78}, α_{79}, and α_{89}	Between nodes on the beam	0.0001	1.000
2	α_{23} and α_{45}	Between nodes on each side of column (except 1 & 6)	0.0005	0.998
3	$\alpha_{27},\alpha_{82},\alpha_{29},\alpha_{37},\alpha_{38},\alpha_{39},\alpha_{47},\alpha_{48},$ $\alpha_{49},\alpha_{57},\alpha_{58},$ and α_{59}	Between nodes on the beam with those on the column (except 1 &6)	0.0012	0.985
4	α_{12}, α_{13}, α_{46},α_{52} and α_{56}	Between nodes on the column	0.0015	0.975
5	$\alpha_{17},\alpha_{18},\alpha_{19},\alpha_{67},\alpha_{68},$ and α_{69}	Between nodes on the beam with those on the column's ends	0.0018	0.967
6	α_{16}	Between two ends of the column	0.0161	0.889
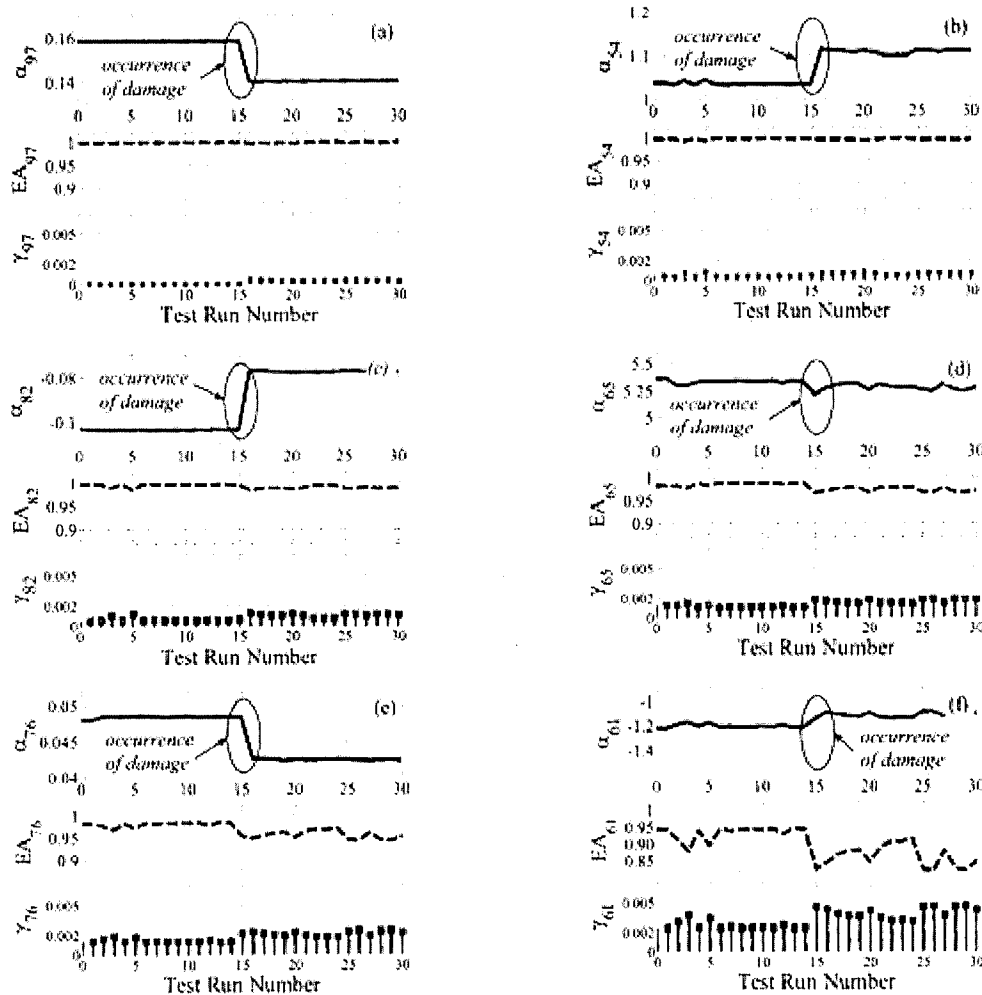
Fig. 5 Pair-wise coefficients (α), estimation accuracy (EA), and evaluation accuracy (γ), for region 1 (a) to region 6 (f)

4.3 Hypothesis testing for significant damage

The difference between undamaged and damaged coefficients can be indicative of the existence and location of damage in a structure. However, in practical scenarios, it is not easy to determine when damage has occurred, and make inferences at different confidence levels. Therefore, another element must be added for complete damage detection: a statistical framework.

The hypothesis testing plot graphically shows the change point of damage, the point at which damage is identified at a certain confidence level, by plotting the test statistic against the test run number. A graph in which the data crosses the confidence bounds, either positive or negative, corresponds to a positive hypothesis, previously defined as H_1 in Eq. (9), indicating the detection of damage. If the accuracy and estimation error associated with the nodes being considered are high and low, respectively, the prediction of the hypothesis test will be more exact and will cross
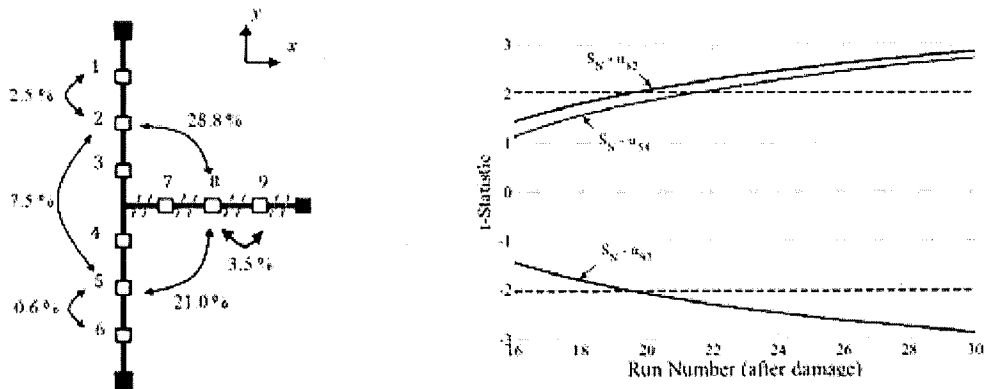
Fig. 6 (a) relative change of some of coefficients and (b) hypothesis testing results for regions 1 to 3

the confidence bounds closer to the occurrence of damage. In order to demonstrate this behavior, the test statistic from the 15 damaged state tests were plotted against their run number. Because damage exists for all of the plotted data, the more accurate damage indicators will yield a plot in which the confidence bounds are crossed closer to the occurrence of damage.

Considering Fig. 6(b), it can be determined that a coefficient with a larger change between the damaged and undamaged states tends to show damage earlier than a coefficient of comparable accuracy with a smaller change. It was shown previously that the region 1 and region 3 coefficients in Table 3 experienced 4-14% and 10-30% average changes, respectively. These parameters cross the bound after only 4 and 5 runs, respectively, whereas, the region 2 coefficients, with 1 to 7% change, take 7 runs to confidently show damage. This suggests that when a statistic crosses the bound first, compared to coefficients of similar accuracy, it is more important to the damage location. Therefore, these plots demonstrate that damage is detected by hypothesis testing, making this method a reliable means of damage detection.

4.4 Comparison of wired and wireless sensor networks

In order to consider realistic application of the proposed damage detection method, there must be a reliable and affordable sensor network with which to instrument the structure. Continued advancements in wireless sensor technology strive to fulfill that role. Deployment of wireless sensor networks (WSNs) is more affordable in terms of manufacturing cost and installation. However, while WSNs make the deployment of SHM more convenient, their possible impact on the reliability and accuracy of the results needs to be assessed (Dorvash and Pakzad 2012). Some challenges in the design of wireless sensor units, such as the trade-off between the functionality and the power consumption, and also attempts for minimizing the cost, cause limitations in their architecture. Literature shows research efforts which present validation of the performance of WSNs through implementations in SHM (Lu *et al.* 2005, 2006, Wang *et al.* 2006, Cho *et al.* 2008). It is however very important to assess the performance of WSNs through comparison of results in SHM applications. In this study, by installing the two wired and wireless sensor networks on the

specimen for simultaneous data collection, direct comparison of result is possible which provides the opportunity to investigate the effects of sensing quality on the performance of the proposed algorithm.

During the tests, data was collected using two previously described sensor networks (wireless and wired). Measured data from each sensor network was analyzed independently. Since the two data acquisition systems worked separately, the data was not automatically synchronized; however, the two sensing networks start measurement at an approximately the same time. By collecting data simultaneously, differences in results due to changes in environmental factors and noise between the two datasets are avoided. Therefore, any differences that appear between the two sets can be attributed to sensing network quality (i.e., performance comparison will reflect the differences corresponding to sensing systems and not different environmental conditions).
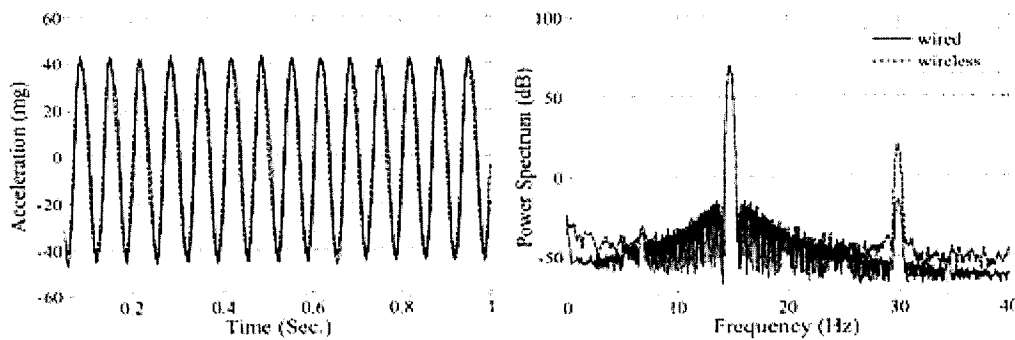

Fig. 7 Comparison of wired versus wireless data in both the time and frequency domains
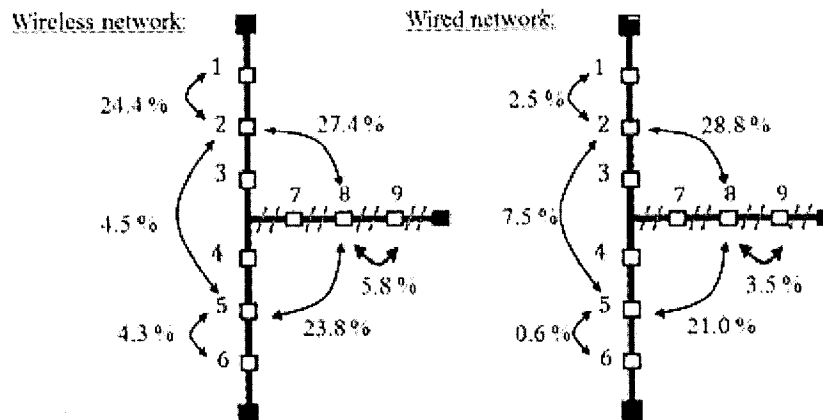

Fig. 8 Comparison of relative change of coefficients between wireless and wired sensor data
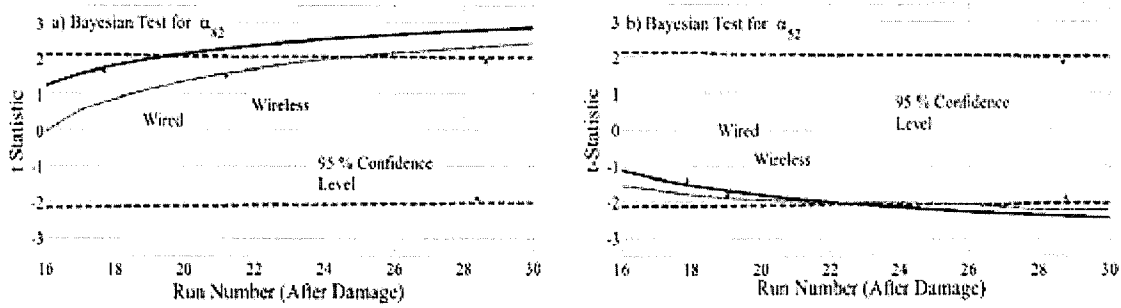
Fig. 9 Comparison of Bayesian Testing Results, wired vs. wireless networks

As the first step for comparison of the performance of the two sensor networks, the collected data from the two are compared in time and frequency domains. Acceleration signals (10,000 samples) are collected at 280 Hz and 250 Hz with the wireless and wired sensors, respectively. Fig. 7 shows a comparison of the data collected at node 9, the node with the largest recorded amplitude. Both wired and wireless signals show the harmonic response due to the harmonic excitation clearly with low visible noise. The frequency content of each sensor type is also comparable; both show a dominant peak at the forcing frequency of 15 Hz. However the wireless data contains more noise at high frequencies as well as at very low frequencies. Note that in creating these plots no digital post-processing (filtering) was performed and the figures show the calibrated recorded signals with the two systems.

Fig. 8 also shows the relative change for selected nodal pairs of the WSN and wired datasets. The changes at α_{85}, α_{82}, and α_{52} of the WSN are comparable to the changes expected from the wired results. The change at α_{89} from the WSN is a bit larger than that of the wired, but still on par with other nodal pairs of its type (beam-beam within damage). On the other hand, a notable inconsistency is seen in two of the column-column nodal pairs, α_{12} and α_{56}. The WSN shows significantly larger changes, almost 10 times larger than those seen in the wired results. This drastic variation can be explained by the EA and γ values of these two coefficients having significantly lower accuracies (less than 0.9) compared to the other four WSN values and the wired values. Lower accuracy correlates to lower reliability. Consequently, these coefficients would not be considered as trusted damage indicators.

A further verification of the algorithm, when using wireless sensors, is obtained via inspection of the hypothesis testing results. The corresponding result for pair-wise coefficient 8-2 and 5-2 is presented in Fig. 9. The first observation from these plots is that the wired sensor system is the first system that identifies the occurrence of damage. This is reasonable based on the higher accuracy associated with wired system compared with this particular WSN in all the results. Fig. 10 shows a direct comparison of influence coefficients α_{82} and α_{52} and their corresponding evaluation accuracy and estimation errors. While both sensor networks reflect the change in the influence coefficients (i.e., indicate the damage), the accuracy of wired sensor results is higher. The performance of wireless sensors, however, is still acceptable since it does detect the damage with 95% confidence level, according to the hypothesis tests, even though this is detected after its detection by the wired system. Based on the presented comparison points it can be seen that the

WSN, while exhibiting higher noise than the wired network, is still effective in localizing the onset of damage. Considering the higher level of noise in the collected data from the wireless sensors (which can be seen in the specification presented in Table 2), the lower accuracy observed in the results of the WSN is reasonable. However, the higher noise in this case could be a worthwhile tradeoff when considering the drastic difference in the cost and implementation difficulties between the two networks.
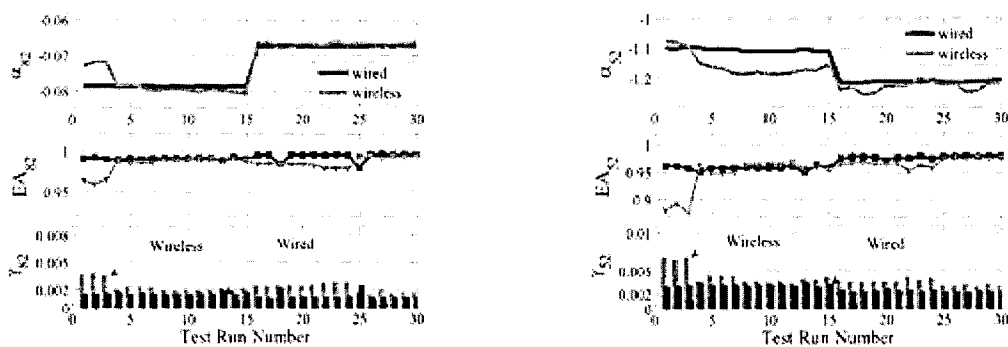

Fig. 10 Comparison of influence coefficient changes, evaluation accuracies and estimation error for two pair-wise nodes (8-2 and 5-2), wired vs. wireless networks

5. Conclusions

An influence-based damage detection algorithm (IDDA) is presented in this paper which is based on regression of the structural response at different locations. The algorithm is integrated with accuracy indicators and a statistical framework to enable evaluation of the significance of the damage as well as estimation of its location, when the damage is detected. To validate IDDA, it is implemented on analytical and experimental models and its performance is evaluated. For the experimental validation, harmonic excitation is selected. However, random excitations for this implementation should be considered in future studies. It is illustrated that the selected damage indicators effectively reflect the structural damage which were simulated in analytical and experimental models. During the implementation of the algorithm on the experimental model, two different networks of wired and wireless sensors with different noise characteristics were utilized. While validating the performance of IDDA, the damage detection resulted from data from each of the two sensor networks were compared and the sensitivity of the algorithm to the sensor characteristics was investigated. The result showed that both sensor networks are able to reflect the change in the influence coefficients and detect damage. However, the accuracy of the wired sensor results was higher, as the noise level of the utilized sensors was lower. The performance of wireless sensors, however, was acceptable as it detected the damage with 95% confidence level, even though it did so later than the wired sensors.

As IDDA is shown to be effective in detecting damage and its location, the future study will be devoted to further investigation of its performance through implementation on large-scale models. Additionally, the embedded processors of the wireless sensors allows for on-board computation

which enables operation of the algorithm on the wireless sensors and providing an automated damage detection system; this task is left for the future work.

Acknowledgments

References

Alvandi, A. and Cremona, C. (2006), "Assessment of vibration-based damage", *J. Sound Vib.*, **292**, 179-202.

Anon. (1992), *ASM handbook, Volume 17, nondestructive evaluation and quality control*, ASM International.

Arici, Y. and Mosalam, K.M. (2003), "Modal analysis of a densely instrumented building using strong motion data", *Proceedings of the International Conference on Applications of Statistics and Probability in Civil Engineering*, San Francisco, CA, June 6-9.

Ball, R.J. and Almond, D.P. (1998), "Detection and measurement of impact damage in thick carbon fibre reinforced laminates by transient thermography", *NDT & E Int.*, **31**(3), 165-173.

Banks, H.T., Joyner, M.L., Wincheski, B. and Winfree, W.P. (2002), *Real time computational algorithms for eddy-current based damage detection*, CRSC-TR01-16, NCSU Inverse Problems 18 795-823.

Bernal, D. (2002), "Load vectors for damage localization", *J. Eng. Mech. - ASCE*, **128**(1), 7-14.

Chang, M. and Pakzad, S.N. (2014), "Observer Kalman filter identification for output-only systems using Interactive Structural Modal Identification Toolsuite", *J. Bridge Eng. ASCE*, **19**(5), 04014002. DOI: 10.1061/ (ASCE)BE.1943-5592.0000530.

Chang, P.C., Flatau, A. and Liu, S.C. (2003), "Review paper: health monitoring of civil infrastructure", *Struct. Health Monit.*, **2**, 257-267.

Chen, J. and Gupta, A.K. (2000), *Parametric statistical change point analysis*, Birkhäuser, Boston

Cho, S., Jo, H., Jang, S., Park, J., Jung, H.J., Yun, C.B., Spencer, Jr., B.F. and Seo, J. (2010), "Structural health monitoring of a cable-stayed bridge using smart sensor technology: data analysis", *Smart Struct. Syst.*, **6**(5-6), 461-480.

Cho, S., Yun, C.B., Lynch, J.P., Zimmerman, A.T., Spencer, Jr., B.F. and Nagayama, T. (2008), "Smart wireless sensor technology for structural health monitoring of civil structures", *Int. J. Steel Struct.*, **8**(4), 267-275

Crossbow Technology, Inc. (2007), *MICAz wireless measurement system*, San Jose, CA.

Deutsch, S. (1979), "A preliminary study of the fluid mechanics of liquid penetrant testing", *J. Res. Natl. Bur. Stand.*, **84**(4), 287-292

Doebling, S.W., Farrar, C.R. and Prime, M.B. (1998), "A summary review of vibration-based damage identification methods", *Shock Vib. Dig.*, **30**, 91-105.

Dorvash, S. and Pakzad, S.N. (2012), "Effects of measurement noise on modal parameter identification", *Smart Mater. Struct.*, **21**(6), 065008.

Dorvash, S., Pakzad, S.N., Naito, C.J., Yen, B. and Hodgson, I.C. (2012), "Application of state of the art in measurement and data analysis techniques for vibration evaluation of a tall building", *J. Struct. Infrastruct. Eng.*, **10**(5), http://dx.doi.org/10.1080/15732479.2012.757795.

Dorvash, S., Pakzad, S.N., Labuz, E.L ., Ricles, J.M. and Hodgson, I.C. (2014), *Localized damage detection*

algorithm and implementation on a large-scale steel beamto-column moment connection, Earthquake Spectra In-Press. doi: http://dx.doi.org/10.1193/031613EQS069M

Farrar, C.R., Allen, D.W., Ball, S., Masquelier, M.P. and Park, G. (2005), "Coupling sensing hardware with data interrogation software for structural health monitoring", *Proceedings of the 6th International Symposium, Dynamic Problems of Mechanics*, Ouro Preto, Brazil.

Farrar, C.R., Baker, W.E., Bell, T.M., Cone, K.M., Darling, T.W., Duffey, T.A., Eklund, A. and Migliori, A. (1994), *Dynamic characterization and damage detection in the I-40 bridge over the Rio Grande*, Los Alamos National Laboratory Report, LA 12767-MS.

Gangone, M.V., Whelan, M.J. and Janoyan, K.D. (2011), "Diagnostic load testing and system identification using wireless sensors", *Comput.-Aided Civil Environ. Eng.*, 26(7), 560-579.

Intel Corporation Research (2005), *Intel Mote2 Overview, Version 3.0* Santa Clara, CA.

Jang, S., Jo, H., Cho, S., Mechitov, K., Rice, J.A., Sim, S.H., Jung, H.J., Yun, C.B., Spencer, Jr., B.F. and Agha, G. (2010), "Structural health monitoring of a cable stayed bridge using smart sensor technology: deployment and evaluation", *Smart Struct. Syst.*, 6(5-6), 439-459.

Jang, S., Jo, H., Cho, S., Mechitov, K., Rice, J.A., Sim, S.H., Jung, H.J., Yun, C.B., Spencer, Jr., B F. and Agha, G. (2010), "Structural health monitoring of a cable stayed bridge using smart sensor technology: deployment and evaluation", *Smart Struct. Syst.*, 6(5-6), 439-459.

Kim, J., Swartz, R.A., Lynch, J.P., Lee, C.G. and Yun, C.B. (2010), "Rapid-to-deploy reconfigurable wireless

Koh, C.G., See, L.M. and Balendra, T. (1995), "Damage detection of buildings: numerical and experimental studies", *J. Struct. Eng. - ASCE*, 121(8), 1155-1160.

Lu, K.C., Wang, Y., Lynch, J.P., Lin, P.Y., Loh, C.H. and Law, K.H. (2005), "Application of wireless sensors for structural health monitoring and control", *Proceedings of the KKCNN Symposium on Civil Engineering*, Taiwan.

Lu, K.C., Wang, Y., Lynch, J.P., Loh, C.H., Chen, Y.J., Lin, P.Y. and Lee, Z.K. (2006), "Ambient vibration study of Gi-Lu cable-stay bridge: application of wireless sensing units", *Proceedings of the SPIE 13th Annual Symposium on Smart Structural and Materials*, San Diego, CA, USA.

Lynch, J.P. and Loh, K.J. (2006), "A summary review of wireless sensors and sensor networks for structural health monitoring", *Shock Vib. Dig.*, 38, 91-128.

Lynch, J.P., Law, K.H., Kiremidjian, A.S., Carryer, E., Farrar, C.R., Sohn, H., Allen, D.W., Nadler, B. and Wait, J.R. (2004), "Design and performance validation of a wireless sensing unit for structural monitoring application", *Struct. Eng. Mech.*, 17(3-4), 393-408.

Mallet, L., Staszewski, W.J. and Scarpa, F. (2004), "Structural health monitoring using scanning laser vibrometry: II. Lamb waves for damage detection", *Smart Mater. Struct.*, 13(2), 261-269.

Morassi, A. and Rovere, N. (1997), "Localizing a notch in a steel frame from frequency measurements", *J. Eng. Mech. - ASCE*, 123(5), 422-432.

Pakzad, S.N., Fenves, G.L., Kim, S. and Culler, D.E. (2008), "Design and implementation of scalable wireless sensor network for structural monitoring", *J. Infrastruct. Eng. - ASCE*, 14(1), 89-101.

Pakzad, S.N. (2008), *Statistical approach to structural monitoring using scalable wireless sensor networks*, PhD dissertation, University of California, Berkeley.

PCB Piezotronics, Inc, (2005), *Single axis capacitive accelerometer*, series 3701, NY.

Ratcliffe, C.P. (1997), "Damage detection using a modified laplacian operator on mode shape data", *J. Sound Vib.*, 204(3), 5-517.

Rice, J.A. and Spencer Jr., B.F. (2008), "Structural health monitoring sensor development for the Imote2 platform", *Proceedings of the SPIE Smart Structures/NDE*, San Diego, CA.

Rice, J.A. and Spencer, B.F. (2009), *Flexible smart sensor framework for autonomous full-scale structural health monitoring*, NSEL Report Series, No. 18, University of Illinois at Urbana-Champaign.

Sen, A. and Srivastava, M.S. (1975), "On tests for detecting change in mean", *Annal. Statistics*, 3, 98-108.

Shahidi, G., Nigro, M.B., Pakzad, S.N. and Pan, Y. (2014), "Local damage features using multivariate regression model", *Struct. Infrastruct. E.*, DOI:10.1080/15732479.2014.949277, In Press.

Sim, S.H., Jang, S.A., Spencer, Jr., B.F. and Song, J. (2008), "Reliability-based evaluation of the

performance of the damage locating vector method", *Probabilist. Eng. Mech.*, **23**(4), 489-495.

Sim, S.H., Spencer, Jr., B.F. and Nagayama, T. (2011), "Multimetric sensing for structural damage detection", *J. Eng. Mech. - ASCE*, **137**(1), 22-30.

Sohn, H. and Law, K.H. (1997), "A Bayesian probabilistic approach for structure damage detection", *Earthq. Eng. Struct. D.*, **26**, 1259-1281.

STMicroelectronics (2005), *LIS3L02AS4 MEMS Inertial Sensor* Geneva, Switzerland.

Straser, E.G. and Kiremidjian, A.S. (1998), *A modular, wireless damage monitoring system for structures*, Technical Report 128, John A. Blume Earthquake Engineering Center, Stanford University, Stanford, CA.

Trimm, M. (2003), "An overview of nondestructive evaluation methods", *J. Fail. Anal.* **3**(3), 17-31.

Wang, Y., Lynch, J.P. and Law, K.H. (2005), "Validation of an integrated network system for real-time wireless monitoring of civil structures", *Proceedings of the 5th Int'l Ws. Structural Health Monitoring*, Stanford, CA, September 12-14.

Whelan, M.J. and Janoyan, K.D. (2009), "Design of a robust, high-rate wireless sensor network for static and dynamic structural monitoring", *J. Intel. Mat. Syst. Str.*, **20**(7), 849-863.

Yao, R. and Pakzad, S.N. (2014), "Damage and noise sensitivity evaluation of autoregressive features extracted from structure vibration", *Smart Mater. Struct.*, **23**(2), 025007. DOI: 10.1088/0964-1726/23/2/025007.

Yoon, M.K., Heider, D., Gillespie Jr., J.W., Ratcliffe, C.P. and Crane, R.M. (2005), "Local damage detection using the two-dimensional gapped smoothing method", *J. Sound Vib.*, **279**(1-2), 119-139.

Yu, Y., Ou, J. and Li, H. (2010), "Design, calibration and application of wireless sensors for structural global and local monitoring of civil infrastructures", *Smart Struct. Syst.*, **6**(5-6), 641-659.

Zilberstein V., Walrath K., Grundy D., Grundya, D., Schlickera, D., Goldfinea, N., Abramovicib, E. and Yentzerc, T. (2003), "MWM eddy-current arrays for crack initiation and growth monitoring", *Int. J. Fatigue*, **25**(9-11), 1147-1155.

BS